2018

Dynamics Study of the Hermetic Compressor

Simone Penazzo
Italia Wanbao-ACC S.r.l., Italy, Simone.Penazzo@wanbao-acc.it

Dynamics Study of the Hermetic Compressor

Simone Penazzo

Italia Wanbao ACC S.r.l., R&D Department
Viale Vasco Salvatelli 4, 32026 Mel (BL), Italy
Phone: 0039 0437 756370, E-mail: Simone.Penazzo@wanbao-acc.it

ABSTRACT

In this Paper a detailed study of dynamics of the hermetic compressor is shown.

The key point of this study is the well-known issue of compressor reciprocating kinematic unbalance which is the main cause of modern refrigerator structural vibrations and consequently acoustical performance. In this frame-work, the main target of this work is the reduction and redistribution of compressor accelerations along "privileged" axes to reduce the aforementioned phenomena.

Starting from the general treatment of Professor Soedel, specific studies on reciprocating kinematic balance are performed. In particular, a detailed model is developed to calculate kinematic forcing terms applying Newton's second law on each component of the reciprocating mechanism. In this model, crankcase reaction forces are equal to kit shaking ones, transmitted to the shell thanks to the suspension springs and the discharge pipe. These shaking forces are redistributed modifying crankshaft mass distribution.

To validate the analytical/numerical models, several vibration and acoustics tests are carried out on variable-speed compressors working both at an un-constrained configuration test and in a load stand at CECOMAF standard conditions. In the first case, cylinder head accelerations are detected in terms of both time series signals and averaged data values, while in the last case, vibrations and acoustic emission are measured on the shell surface and particularly near to suction and delivery ducts. Different test ensembles are completed modifying single kit components in the frame of the DOE approach.

Experimental results match with theoretical predictions in terms of both vibration reduction and redistribution along reference axes for all the tested displacements, with beneficial effects on compressor acoustics too. Furthermore, the developed software reveals to be a useful research tool for product update, simplification and innovation.

1. INTRODUCTION

Recently, refrigerator noise has gained more and more importance since it is strongly related to the acoustic comfort of daily life. In all refrigerators, noise is caused by reciprocating compressor vibrations, which are transmitted to the surrounding structure via connection flanges, connecting suction/discharge tubes and working fluid pulsations (only in the case of refrigerator piping resonances).

In detail, compressor vibrations are caused by electric motor magnetic forces, gas pulsations (due to the periodical compression phase), unbalance of translating and/or rotating devices (conrod, piston, rotor for a 1-cilynder compressor) and impulsive forces triggered by valve impacts (Soedel, 2006, Trella and Soedel, 1972, Hamilton, 1988).

In modern refrigerators, application noise is strongly related to connecting suction/discharge tube vibrations which can be optimized working on the reciprocating compressor balance in terms of vibration distribution along its reference axes. In this frame, it is well known (i.e. (Soedel, 2006)) the characteristic unbalance of 1-cylinder reciprocating compressors along the piston motion direction (named x axis) with respect to the orthogonal direction (named y axis)

in the same horizontal plane. This unbalance is detrimental for modern refrigerator acoustics since flexural vibration modes can be exited with possible resonant effects on the least stiff components.

According to the previous reasoning, this work aims at modifying the unbalance of 1-cylinder compressors shifting (part of) x axis acceleration to y axis one. One possibility is the modification of crankshaft counterweight mass distribution: in this work, two different cases have been created adding known masses in precise positions (Figure 1):

Figure 1: Counterweight mass addition. Balance n°1 on the left, n°2 on the right

To determine the best new balance, compressor vibrations have been measured on different points of its assembly: first on the cylinder head (open un-constrained compressor test, named test 1, see Figure 2) and then on the external shell (named test 2, based on ISO 3745 measurement in a semi-anechoic room according to CECOMAF GT4-008 standard conditions, see Figure 3).

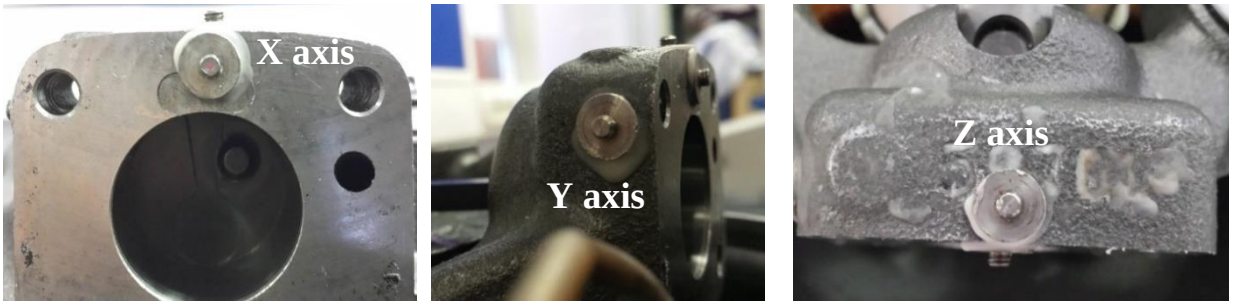

Figure 2: Positions of the accelerometers glued on the cylinder head (test 1).

Figure 3: Positions of the accelerometers on the external shell (test 2).

The balance demonstrating the best compromise between compressor noise and shell vibrations has been selected for application noise measurements in a reverberant room environment. In this work, the results of only 1 displacement (9.5 cm^3) are reported. At the same time, test-1 theoretical calculations have been carried out to perform parametric studies on different added masses in different displacements.

2. THEORETICAL MODEL

The slider-crank mechanism can be schematized as the following (out-of-scale) picture:

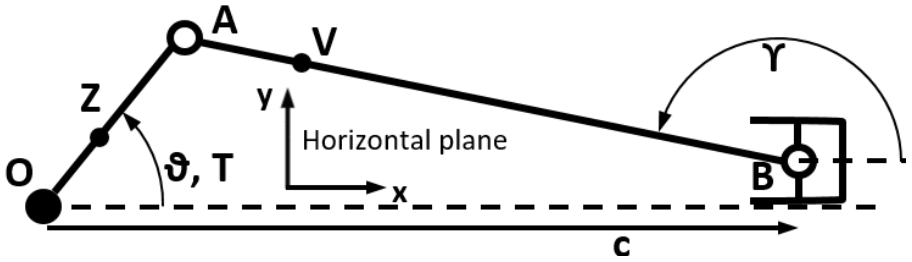

Figure 4: Slider-crank kinematic scheme

In Figure 4, it is possible to distinguish the crankshaft-rotor assembly (O fixed rotation hinge, Z: center of gravity, OZ < 0 due to the counterweight), its eccentricity (OA), the conrod (AB, V: center of gravity), the conrod-piston joint (B) and the piston stroke **c**.

The theoretical model involves rigid bodies, perfect joints (no wear, no clearances), constant crankshaft angular velocity (no transient phases), planar kinematics (no z forces exiting this paper plane), rotor perfectly balanced and no friction losses at each contact surface.

After having solved the kinematics (**ϑ, ϒ, c** and their time derivatives), force equilibrium equations are written for each body along x and y direction (9 equations) applying Newton's 2nd Law. Piston pressure can be inserted into the model to calculate the instantaneous torque (T) necessary to have a constant $\dot{\theta}$ angular velocity. However, in vibration calculations, piston pressure is an internal force and so this passage is omitted. The reaction forces exchanged by the crankcase and the slider-crank mechanism are shaking forces transmitted to the shell thanks to the suspension springs and the internal discharge tube. The counterweight mass contribution is modeled using 2 degrees of freedom characterizing univocally the added static moment (S and Δ parameters, $S \geq 0$, $0 \leq \Delta \leq 360°$) as reported in Figure 5:

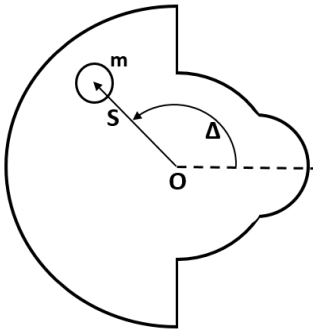

Figure 5: Counterweight mass addition simulation

In the same model, common conrod dynamics approximations (2-mass conrod, 3-mass conrod) are not used since conrod barycenter coordinate data are easily available from CAD models.

3. CALCULATIONS

An Excel sheet has been generated to solve the previous equations. Useful graphs can be generated at different running velocities for the same displacement. In Figures 6-7, the theoretical effect of counterweight mass addition on kit accelerations is clearly visible (the highest added static moment is due to balance n°2).

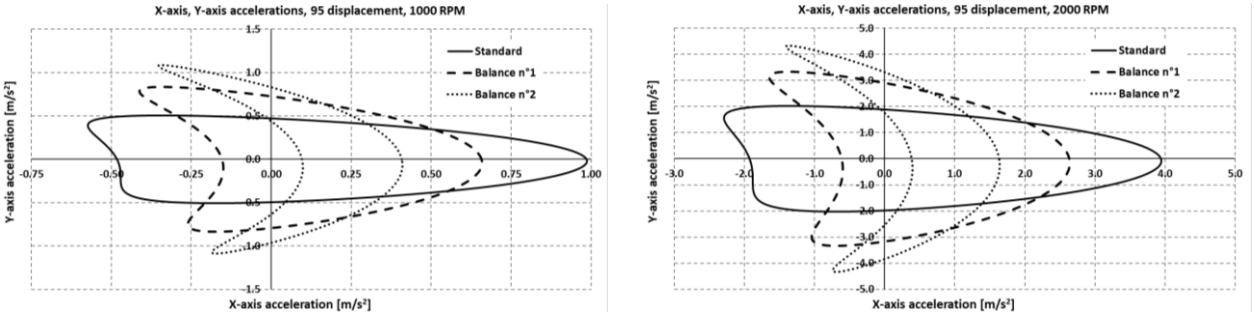

Figure 6: x-, y-axis kit accelerations for a 9.5 cm^3- displacement VSD compressor at 1000 and 2000 RPM

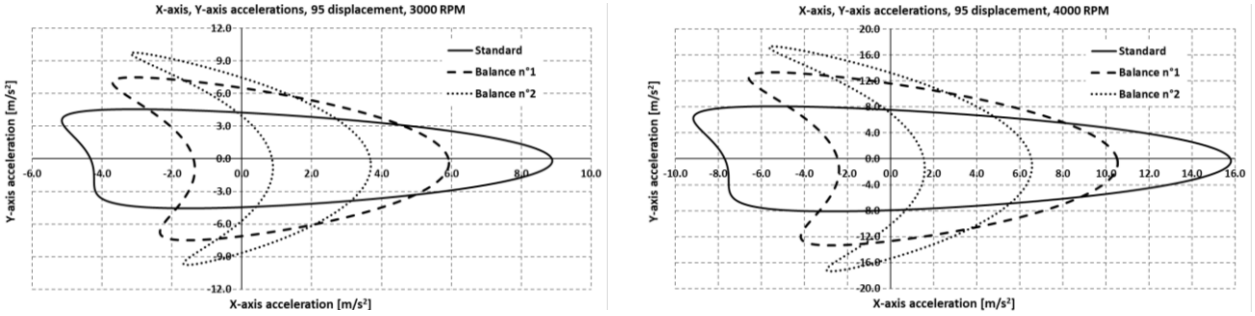

Figure 7: x-, y-axis kit accelerations for a 9.5 cm^3- displacement VSD compressor at 3000 and 4000 RPM

The same theoretical curves (Figure 8) have been generated for a lower displacement sharing the same counterweight:

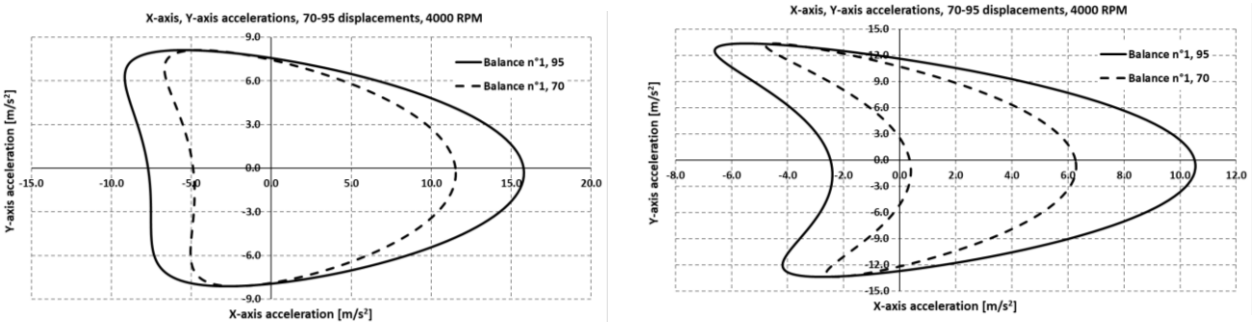

Figure 8: x-, y-axis kit accelerations comparison between 9.5 cm^3- and 7 cm^3 - displacements at 4000 RPM. Standard balance (STD, left), balance n°1 (right).

In the lower displacement, the lower piston mass (-23%) is responsible for a more regular standard balance.

In Figures 6-8, each curve starts from x axis (crankcase rotation = 0°) and it is covered in anti-clockwise direction. All the curves are not symmetrical (particularly x-axis ones): this is caused by the crankcase barycenter placed near the cylinder head.

4. EXPERIMENTAL RESULTS

The following graphs report examples of 9.5 cm^3-displacement x- and y-axis head cylinder acceleration time acquisitions (test 1) of all the tested balances at different velocities:

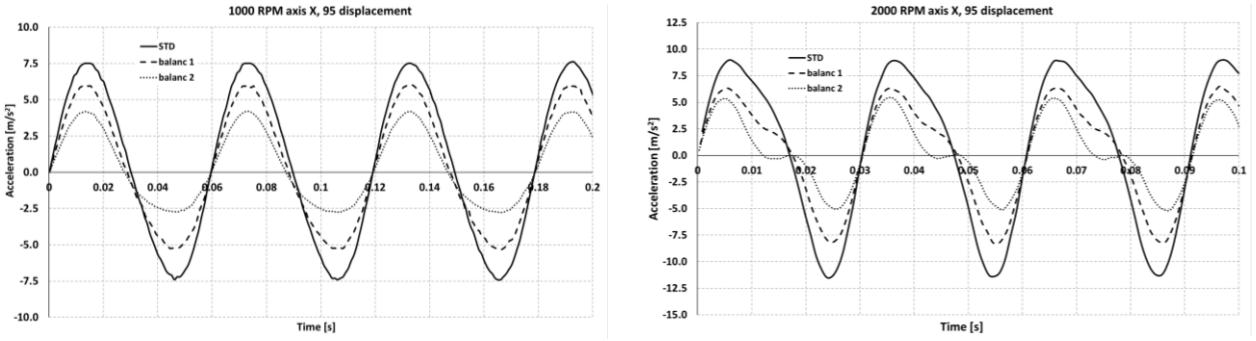

Figure 9: x-axis experimental accelerations measured on the cylinder head at 1000, 2000 RPM

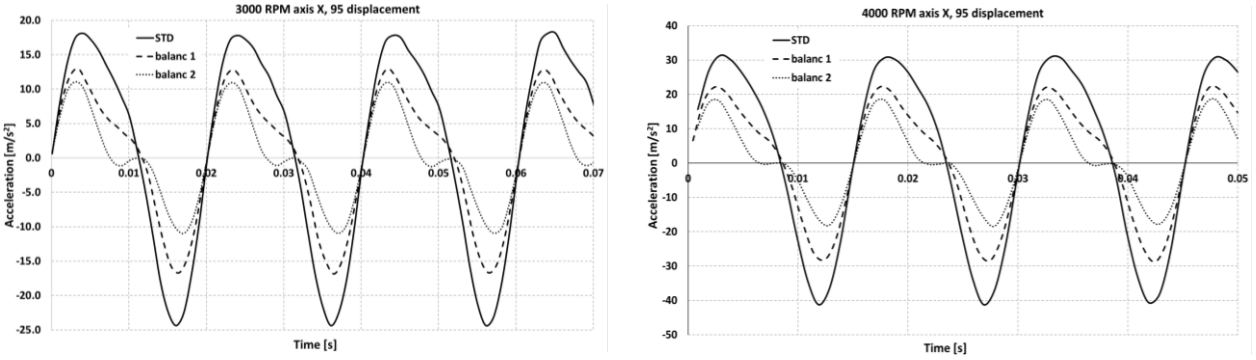

Figure 10: x-axis experimental accelerations measured on the cylinder head at 3000, 4000 RPM

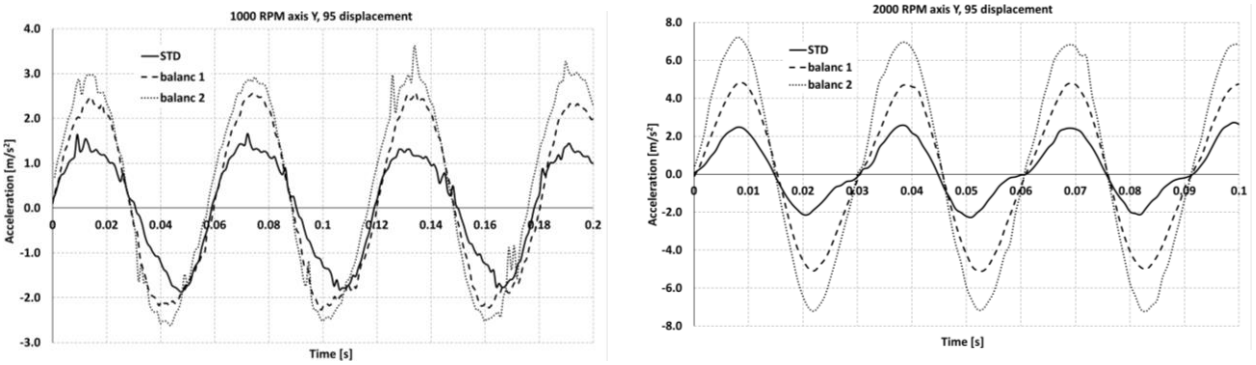

Figure 11: y-axis experimental accelerations measured on the cylinder head at 1000,2000 RPM

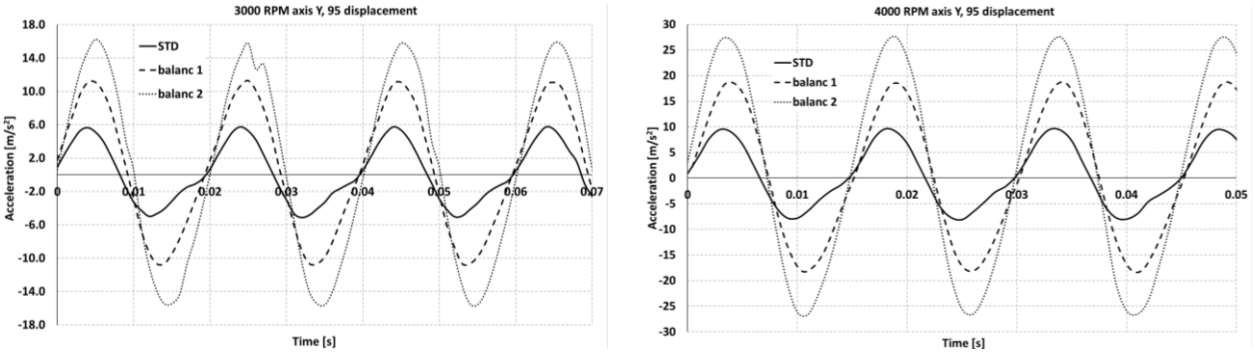

Figure 12: y-axis experimental accelerations measured on the cylinder head at 3000, 4000 RPM

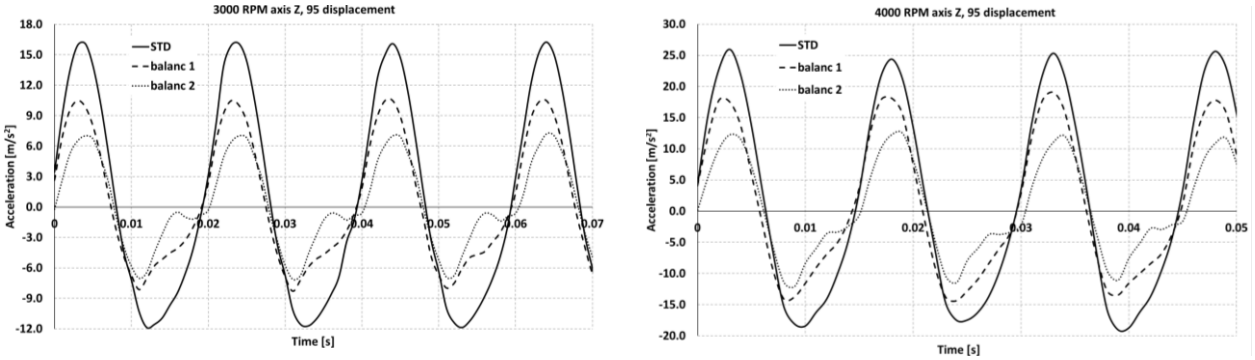

Figure 13: z-axis experimental accelerations measured on the cylinder head at 3000, 4000 RPM

About z axis, only 2 graphs (at 3000 and 4000 RPM) are showed for the sake of simplicity. In these 2 graphs, it is possible to appreciate the reduction of Z-axis acceleration due to acceleration shifting from x to y axis.

A complete view of the new balance positive results is appreciable analyzing Tables 1-3, where compressor shell vibration (Tables 1-2) and acoustic tests (test 2, Table 3) have been completed on the 9.5-cm^3 displacement model. Uncertainty is calculated using the t-Student distribution with a confidence interval of 95%.

Table 1: Average TVI at different velocities of all the investigated balances.

Average TVI [mm/s] (shell measurements, test 2)			
RPM	**STD balance**	**Balance n°1**	**Balance n°2**
1000	1.84 ± 0.31	0.97 ± 0.27	1.11 ± 0.33
2000	0.49 ± 0.04	0.87 ± 0.35	1.14 ± 0.23
3000	0.85 ± 0.13	0.53 ± 0.17	0.47 ± 0.17
4000	1.63 ± 0.21	0.99 ± 0.17	1.04 ± 0.53

Table 2: Table-1 detailed vibration data at different velocities of all the investigated balances.

	STD balance			**Balance n°1**			**Balance n°2**		
RPM	**% X**	**% Y**	**% Z**	**% X**	**% Y**	**% Z**	**% X**	**% Y**	**% Z**
1000	50.6	39.7	9.7	40.1	45.5	14.4	33.0	51.9	15.0
2000	46.5	32.6	21.0	3.8	93.5	2.7	4.1	94.0	1.9
3000	63.3	1.4	35.3	37.0	43.5	19.5	43.6	27.0	29.3
4000	18.3	2.0	79.7	9.3	44.6	46.1	9.6	20.8	69.6

On Table 2, since TVI is a 3D vector, each acceleration percentage has been calculated according to the following equations:

$$\%\, X = 100 \cdot \left(\frac{v_x}{TVI}\right)^2; \quad (1)$$

$$\%\, Y = 100 \cdot \left(\frac{v_y}{TVI}\right)^2; \quad (2)$$

$$\%\, Z = 100 \cdot \left(\frac{v_z}{TVI}\right)^2; \quad (3)$$

$$\sqrt{\left(\frac{v_x}{TVI}\right)^2 + \left(\frac{v_y}{TVI}\right)^2 + \left(\frac{v_z}{TVI}\right)^2} = 1; \quad (4)$$

Table 3: Average LWA at different velocities of all the investigated balances.

Average LWA [dBA]			
RPM	**STD balance**	**Balance n°1**	**Balance n°2**
1000	30.9 ± 1.8	30.3 ± 1.1	36.7 ± 5.0
2000	35.7 ± 1.1	36.4 ± 2.7	40.6 ± 3.4
3000	39.0 ± 0.6	39.2 ± 1.5	42.2 ± 2.4
4000	43.1 ± 0.5	42.9 ± 1.6	45.0 ± 2.8

In the standard (STD) balance, Z-axis acceleration component has a monotonical increasing trend as velocity increases while for the other components, the highest velocities (3000-4000 RPM) show the worse balance (1.4% and 2.0% of y-axis acceleration). At lower velocities, the kit resonance is probably responsible for a more equal balance between x and y direction.

About LWA results, balance n°1 is equivalent to standard one considering the experimental deviation. Conversely, balance n°2 suffers from enhanced noise emission maintaining a TVI lower than standard balance one: probably, the enhanced noise is due to shell higher modes placed out of the vibrations measurement range (16-800 Hz).

To conclude, some vibration and acoustic spectra (shell measurements, test 2) of 1 compressor of each tested balance are reported in Figures 14-16:

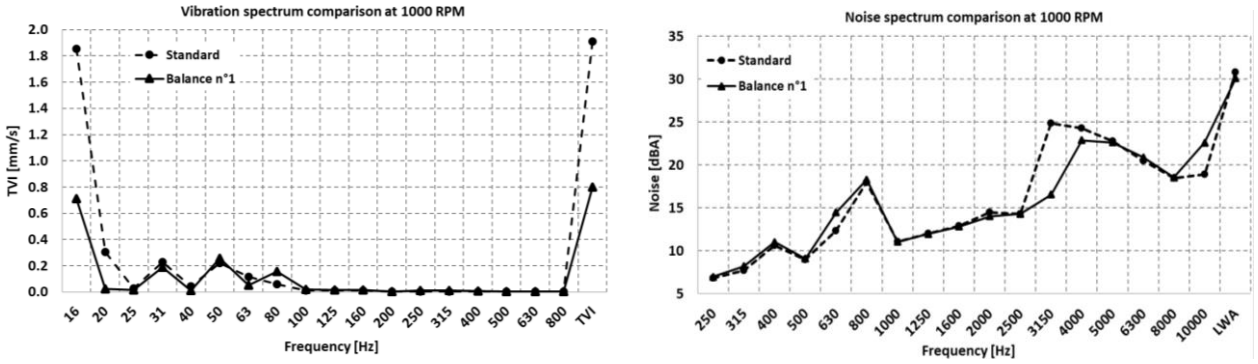

Figure 14: 1000-RPM vibration and noise spectra of 1 compressor of Tables 1-3

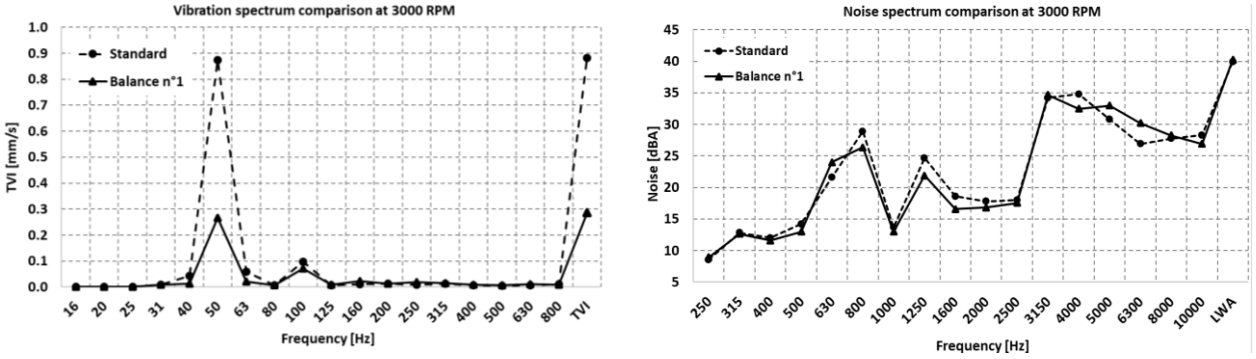

Figure 15: 3000-RPM vibration and noise spectra of 1 compressor of Tables 1-3

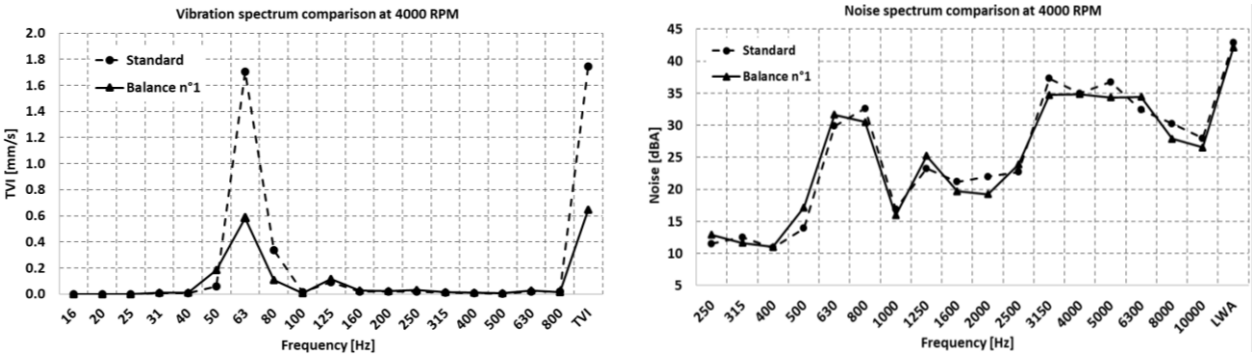

Figure 16: 4000-RPM vibration and noise spectra of 1 compressor of Tables 1-3

Final application noise tests (reverberant room) have been carried out on the same compressors of Figures 14-16 at estimated speeds in the range 2450-2550 RPM. Two working conditions have been tested: 35-minute cycle (refrigerator + freezer working simultaneously), 25-minute cycle (refrigerator only) Each curve is the average of 2 runs. Results are reported in Figures 17-18 and Tables 4-5:

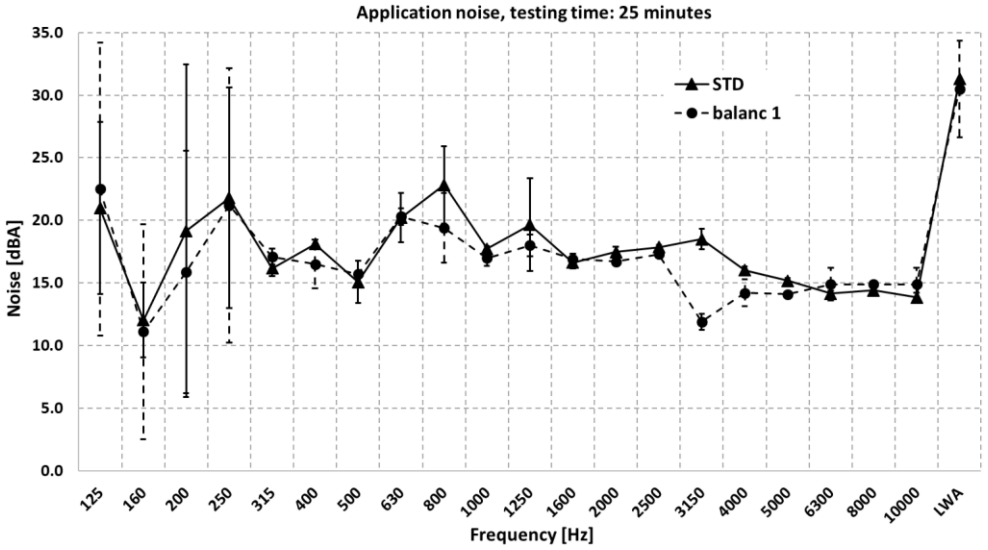

Figure 17: 25-minute application noise results of standard and modified compressor balance (n°1)

Table 4: Tabular data of Figure 17

[Hz]	Standard	n°1	Δ [dBA]	[Hz]	Standard	n°1	Δ [dBA]
125	21.0	22.5	1.5	1600	16.6	16.9	0.3
160	12.0	11.1	-0.9	2000	17.5	16.7	-0.8
200	19.2	15.9	-3.3	2500	17.8	17.3	-0.5
250	21.8	21.2	-0.6	3150	18.5	11.9	-6.6
315	16.2	17.1	0.9	4000	16.0	14.2	-1.8
400	18.1	16.5	-1.6	5000	15.2	14.1	-1.1
500	15.1	15.7	0.6	6300	14.2	14.9	0.7
630	20.2	20.3	0.1	8000	14.4	14.9	0.5
800	22.8	19.4	-3.4	10000	13.9	14.9	1.0
1000	17.7	17.0	-0.7	**LWA**	**31.3**	**30.5**	**-0.8**
1250	19.6	18.0	-1.6				

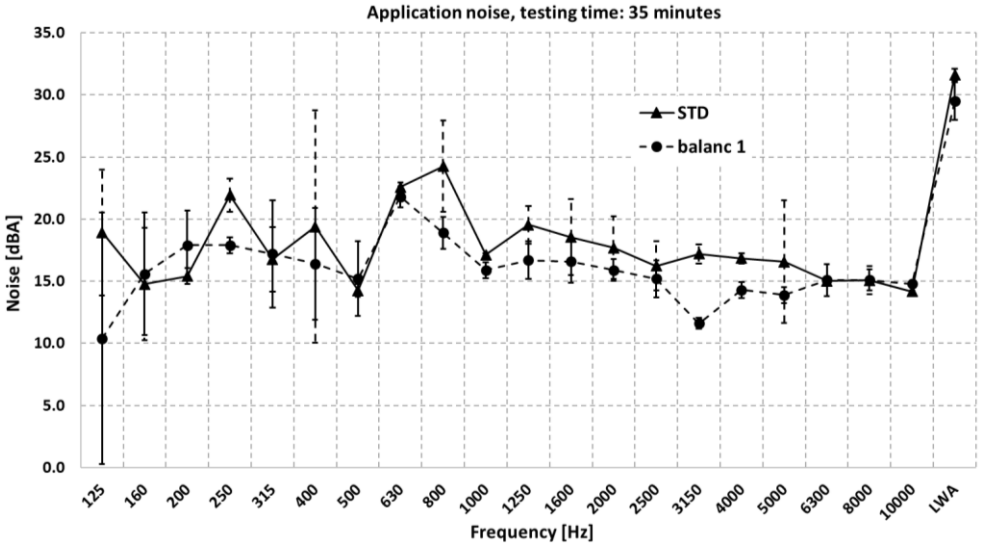

Figure 18: 35-minute application noise results of standard and modified compressor balance (n°1)

Table 5: Tabular data of Figure 18

[Hz]	Standard	n°1	Δ [dBA]	[Hz]	Standard	n°1	Δ [dBA]
125	18.9	10.4	-8.5	1600	18.5	16.6	-1.9
160	14.8	15.6	0.8	2000	17.7	15.9	-1.8
200	15.4	17.9	2.5	2500	16.2	15.2	-1.0
250	21.9	17.9	-4.0	3150	17.2	11.6	-5.6
315	16.8	17.2	0.4	4000	16.9	14.3	-2.6
400	19.4	16.4	-3.0	5000	16.6	13.9	-2.7
500	14.3	15.2	0.9	6300	15.0	15.1	0.1
630	22.6	21.8	-0.8	8000	15.1	15.1	0.0
800	24.3	18.9	-5.4	10000	14.2	14.8	0.6
1000	17.1	15.9	-1.2	**LWA**	**31.6**	**29.5**	**-2.1**
1250	19.5	16.7	-2.8				

In the longest application test (35 minutes), LWA reduction of about 2 dBA is reached thanks to the smoothing of spectrum peaks at the frequencies 250, 400, 800 and 3150 Hz. In both the application tests, an appreciable noise reduction is reached in the 3150-Hz band which is directly associated with reduced compressor shell high-frequency modes amplitude.

5. CONCLUSIONS AND NEXT STEPS

In this work, an approach to modify the balance of a 1-cilynder reciprocating compressor is proposed. The aim of this new balance is to lower application noise by reducing compressor shell vibrations. Vibration and acoustic tests on compressors and refrigerators confirm the validity of this approach for the investigated range of speeds. Similar results have been obtained also for lower displacements. Furthermore, this model can be used to estimate mass production variability due to counterweight tolerances dispersion.

Possible future developments of this work consist in a detailed study of vibration transmission from the kit to the external shell. In this case, it could be possible to reduce vibration transmission optimizing internal discharge tube and suspension springs transmissibility curves changing several geometrical parameters and using elastic materials with appreciable internal damping. Otherwise, it is possible to modify foot straps stiffness changing either their shape or their welding points which are extremely important for high-frequency shell mode shapes and frequencies.

NOMENCLATURE

VSD	Variable – Speed Driver	(-)
LWA	Overall noise level	(dBA)
STD	Standard	(-)
Δ	Delta (Difference between two quantities)	(-)
TVI	Total Velocity Index	(mm/s)
v_x, v_y, v_z	TVI components along x, y, z axes respectively	(mm/s)

REFERENCES

1. Soedel, W. (2006). *Sound and vibrations of positive displacement compressors*. CRC press.
2. Trella, T. J., & Soedel, W. (1972). On Noise Generation of Air Compressor Automatic Reed Valves.
3. Hamilton, J. F. (1988). Measurement and control of compressor noise. *West Lafayette, USA: Purdue University*.

ACKNOWLEDGEMENTS

The author would like to thank Dr. Fabio Giusto for his consultancy contributions.